Microsc. Microanal. 21, 1314–1326, 2015
doi:10.1017/S1431927615015019

Microscopy AND Microanalysis

Microscopy Characterization of Silica-Rich Agrowastes to be used in Cement Binders: Bamboo and Sugarcane Leaves

Josefa Roselló,[1] Lourdes Soriano,[2] M. Pilar Santamarina,[1] Jorge L. Akasaki,[3] José Luiz P. Melges,[3] and Jordi Payá[2,*]

[1]*Departamento de Ecosistemas Agroforestales, Universitat Politècnica de Valéncia, E-46022 Spain*
[2]*Instituto de Ciencia y Tecnología del Hormigón ICITECH, Universitat Politècnica de Valéncia, E-46022 Spain*
[3]*UNESP - Univ Estadual Paulista, Departamento de Engenharia Civil, Campus de Ilha Solteira, SP CEP 15385-000, Brasil*

Abstract: Agrowastes are produced worldwide in huge quantities and they contain interesting elements for producing inorganic cementing binders, especially silicon. Conversion of agrowastes into ash is an interesting way of yielding raw material used in the manufacture of low-CO_2 binders. Silica-rich ashes are preferred for preparing inorganic binders. Sugarcane leaves (*Saccharum officinarum*, SL) and bamboo leaves (*Bambusa vulgaris*, BvL and *Bambusa gigantea*, BgL), and their corresponding ashes (SLA, BvLA, and BgLA), were chosen as case studies. These samples were analyzed by means of optical microscopy, Cryo-scanning electron microscopy (SEM), SEM, and field emission scanning electron microscopy. Spodograms were obtained for BvLA and BgLA, which have high proportions of silicon, but no spodogram was obtained for SLA because of the low silicon content. Different types of phytoliths (specific cells, reservoirs of silica in plants) in the studied leaves were observed. These phytoliths maintained their form after calcination at temperatures in the 350–850°C range. Owing to the chemical composition of these ashes, they are of interest for use in cements and concrete because of their possible pozzolanic reactivity. However, the presence of significant amounts of K and Cl in the prepared ashes implies a limitation of their applications.

Key words: agrowaste, silica, phytolith, pozzolan, spodogram

Introduction

The generation and management of waste is an issue of vital importance for economic and environmental development, and has direct implications for sustainability in the XXI century. Valorization of wastes consists of converting them for producing energy, fuels, chemicals, and other useful products. Valorization puts the emphasis on environmental indicators and sustainability goals (Nzihou, 2010). Of all the wastes generated, those that occupy the greatest volume are related to primary activities, specifically farming and forestry. The recovery of such waste is focused in certain cases on the preparation of agricultural feed for livestock. In addition, many recent studies have assessed the great potential for applying specific crops to chemical production (Tuck et al., 2012).

Because of the volume of crops produced worldwide, strategies focused on high-consumption practices may be developed. In this sense, the construction sector is of great interest because it is the human activity in which the most tons of materials are processed. Thus, interesting approaches for producing vegetable fibers as nonconventional reinforcement for construction materials (cement- or polymer-based) are being developed (Santos et al., 2015). However, only a small part of biomass can be converted into useful fibers; in other cases, valorization in alternative sectors is not possible because the presence of some elements in the biomass or the transport distances do not permit viable technical solutions.

In that case (Payá et al., 2010), it is possible to carry out a first valorization (first stage, Fig. 1) through the recovery of energy by combustion processes in which a secondary material, the ash residue, is generated. Ashes can be valued at a later stage (second stage, Fig. 1): depending on the chosen option, different valorization levels can be achieved. The lowest valorization level corresponds to landfill (no recovery); the highest levels correspond to the use of these ashes as mineral additions for manufacturing cement and concrete. In some cases, the ash obtained is rich in silicon, which is of crucial interest in the field of high performance concrete: amorphous silica (SiO_2) has pozzolanic properties, that is, the capacity for chemical combination with portlandite released in the hydration of Portland cement to form cementitious materials of insoluble character (Mehta, 1989). These ashes could compete with microsilica, a byproduct from the silicon and ferrosilicon alloy industries, which has become a high-added value mineral addition in the concrete sector: this microsilica is very expensive and its production is limited to only a few countries. Thus, the production of high-reactive pozzolans from biomass is an interesting issue for many countries, mainly for developing ones.

Plants absorb silicon from the soil as silicic acid which is deposited as amorphous hydrated silica or opal ($SiO_2.nH_2O$)

Received May 8, 2015; accepted July 22, 2015
*Corresponding author. jjpaya@cst.upv.es

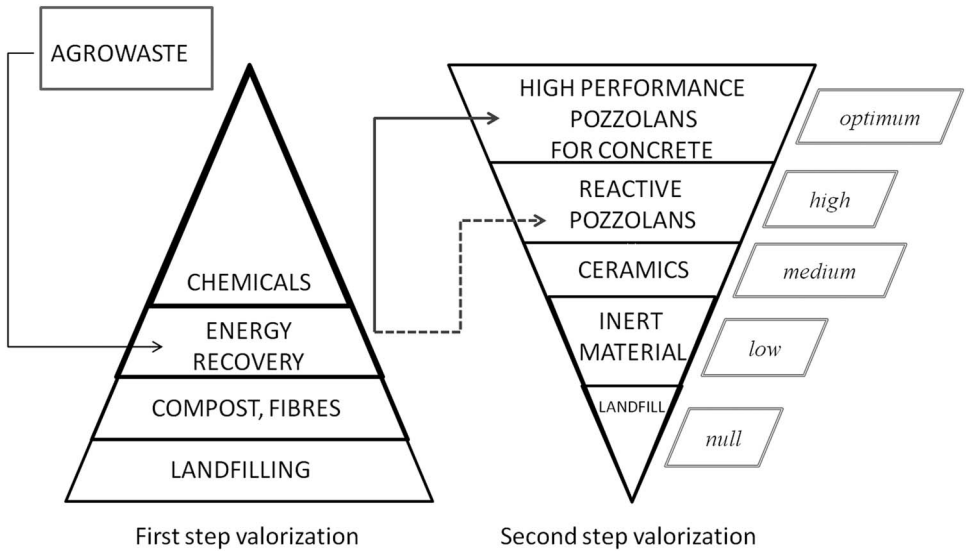

Figure 1. Valorization steps and levels for agrowaste.

in the cell wall, inside the cells (intracellular spaces or cell lumen) and in the intercellular spaces of different plant organs such as leaves, pods, stems, inflorescences (i.e., herringbones), and epidermal appendages (trichomes) (Prychid et al., 2003).

Silica content is between 0.1 and 10% dry weight of higher plants. In general, monocots accumulate more silica than dicots, although there may be differences even to the genus level (Ma & Yamaji, 2006). Among monocots, the Poaceae family (grasses) accumulate much more silica in the cellular tissues than other families of plants.

Different siliceous structures have been found in plants. There are special siliceous cells that are called phytoliths or silico-phytoliths. After the death of the plant, these qphytoliths are preserved in the soil for hundreds or thousands of years and can therefore be used to understand the interrelationships that occurred between plants, ecosystems, and ancient human communities. In addition, these siliceous structures occluded some organic carbon when formed during plant growth and play an important role in the long-term carbon sink of ecosystems (Li et al., 2014).

Silicon has an important role in plant–environment relationships, and confers resistance and protection against various biotic and abiotic environmental factors. The accumulation of silica provides mechanical stability to the tissues, reduces water loss through transpiration (resistance to water stress), reduces problems caused by lack of or excess nutrients, and protects the plant against attack by insects and microorganisms, thereby reducing infections caused by them (Epstein, 1999).

A wide variety of phytolith shapes can be found (Erra et al., 2011) and most of them are $<50\,\mu$m in size. Their shape depends on the plant tissue in which the silica was deposited and the intracellular space thereof. The most characteristic phytoliths have the following morphotypes: dumbbell, saddle, and cross. In the case of extracellular deposits, in external plant tissues (epidermis), trichomes are the most typical.

The epidermis of Poaceae family plants has taxonomic value, and therefore the most important cellular elements are used as diagnostic characteristics: silica cells (phytoliths), cork cells, and trichomes (bicellular, unicellular, papillose). These elements have structural value and their presence and distribution permit the classification of plants in differentiated sub-families. There are different classifications of siliceous bodies, and three different dermotypes in grasses can be distinguished (Fig. 2) according to Prat (1936).

(a) Panicoide dermotype: characterized by bilobated silica cells (dumbbell shape) and bicellular trichomes in different forms (e.g., sugarcane); (b) Festucoide dermotype: rounded or elongated silica cells with slightly wavy walls, trichomes, if present, are unicellular (e.g., festuca, hay); and (c) Bambusoide dermotype: silica cells of various shapes (dumbbell and saddle) and unicellular (prickle) and bicellular (filiformed) trichomes (e.g., bamboo and guadua).

Few studies have been performed on the chemical composition of phytoliths. Kamenik et al. (2013) studied phytoliths from barley (festucoid type), and they found a silica content of 84.8% for phytoliths in the leaf and 89.8% for those present in the stem.

The presence of silica in agrowaste and then in the ashes produced by its combustion is of great interest for several fields including ceramics (Mohapatra et al., 2011; Teixeira

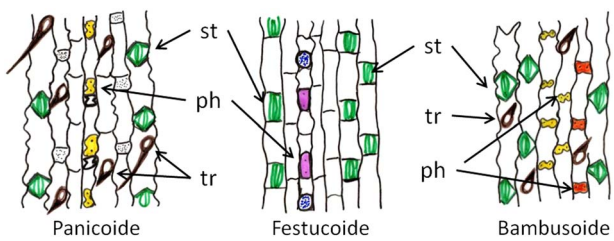

Figure 2. Dermotypes found in leaves of Poaceae family plants. ph, phytolith; st, stoma; tr, trichome.

et al., 2014) and nanotechnology (Neethirajan et al., 2009). However, the most important field for utilizing this type of ash is the cement and concrete industry. Research on the use of ash from agricultural waste in the manufacture of cement (biocements) has increased in recent years (Hosseini et al., 2011). Rice husk ash has been the most studied (Aprianti et al., 2015) waste: its chemical composition reveals that silica is the major compound, in excess of 92–93% by weight based on ignited samples (without carbon or organic matter) (Payá et al., 2010). In other cases, the SiO_2 content in the ash is lower. For example, a large amount of silica has been found (Hosseini et al., 2011) in ashes from sugarcane straw (59%), sawdust (67%), corncob (66%), oil palm shell (63%), wheat straw (54%), and bamboo leaf (BL) (76%).

Many of these ashes were tested (Aprianti et al., 2015) from the viewpoint of reactivity with Portland cement and/or hydrated lime, and their pozzolanic activity was determined by means of mechanical tests and/or physico-chemical tests (thermogravimetry, electrical conductivity, X-ray diffraction, microscopy, etc.). Furthermore, in some cases the durability properties of concretes containing biomass ashes have been assessed. In cement chemistry, it is crucial to know the nature of individual particles in order to study their reactivity (e.g., hydration process and/or pozzolanic reaction process). This is because the reactions involve a heterogeneous system (liquid/solid, e.g., water/cement + pozzolan), and each individual particle could produce specific reaction compounds.

The aim of this research is to study in depth from the microscopic point of view the plant structures and ashes obtained from bamboo leaves and sugarcane leaves (SL), in order to analyze the silica distribution and presence of other compounds, and also the presence of silica bodies (phytoliths). Thus, selected information about the chemical nature of ashes will be obtained, which is interesting for further studies in Portland cement blends (ashes acting as pozzolans). Both bamboo and SL are residues from several industries. Specifically, bamboo leaves are produced in huge amounts because this is probably the fastest-growing and highest yielding natural resource and construction material available to mankind (Asha et al., 2014). The use of bamboo cane and its fibers generates solid waste (mainly leaves and short stems). The same occurs in sugarcane harvesting. The burning of this biomass in open landfills (Le Blond et al., 2008) has a negative impact from the environmental point of view, producing smoke and very dangerous airborne particles.

Methods and Materials

Leaf samples of bamboo (*Bambusa vulgaris*, BvL and *Bambusa gigantea*, BgL) and sugarcane (*Saccharum officinarum*, SL) were collected in Ilha Solteira (São Paulo, Brazil). Old leaves were taken from the plant because silicon is an element accumulated along the life of the plant, and it is not moved to other parts of the plant once deposited as silica (Ma & Yamaji, 2006). To correctly identify structures rich in silica (phytoliths) and their location within the plant, studies on both collected material (fresh and dried) and ash resulting from combustion in a muffle furnace at selected temperatures were performed. Leaves were previously washed with deionized water. Small pieces of the leaves were cut from the center part.

Preparation of samples was carried out depending on the type of study. For fresh material studies, leaf samples of bamboo and sugarcane were washed thoroughly to remove residual soil contamination. Sections were cut into 1 cm^2, and paradermal lamellae of 40-μm thick were prepared using a freezing microtome (Jung AG, Heidelberg, Germany). Subsequently these cuts were clarified with a solution of 50% sodium hypochlorite and washed several times with distilled water. For dried material studies, small samples of leaves were dried at 105°C for 24 h in a laboratory oven (UN model; Memmert, Schwabach, Germany). For calcined material (ash), fresh samples were calcined for 1 h at the selected temperature (350, 450, 550, or 850°C; these temperatures were selected in terms of stability of the spodogram) in a muffle furnace (RHF model 1500; Carbolite, Hope Valley, UK). The obtained ashes were: bamboo leaf ash (BLA) (from *B. vulgaris*, BvLA; from *B. gigantea*, BgLA) and sugarcane leaf ash (SLA).

Optical microscopy (*OM*): the cuts of fresh material, once clarified, were stained with safranin-light green, dehydrated, and mounted using a synthetic mix of resins (Eukitt, Sigma-Aldrich, San Luis MO, USA; mounting medium for microscope preparation) for observation under a light microscope (Olympus PM-10AK3, Tokio, Japan).

Cryo-scanning electron microscopy (*SEM*): clarified cuts (fresh material) were frozen in liquid nitrogen and transferred to a cryo-transfer system (CT-1000C, Oxford Instruments, Oxford, UK) interconnected with a SEM (JEOL JSM-5410, Oxford Instruments, Oxford, UK). The sample was sublimed at −90°C and once coated with gold the structure was analyzed by SEM.

SEM: selected samples (dried leaves and ashes) were coated with carbon (Baltec SCD 005 evaporation supply CEA, Zurich, Switzerland) and then analyzed with a SEM (JEOL JSM-6300, Oxford Instruments, Oxford, UK) equipped with energy-dispersive X-ray (EDX) for microanalysis. As the sample is formed by interconnected particles and is highly porous with a nonpolished surface, EDX analyses must be considered from the semiquantitative point of view.

Field emission scanning electron microscopy (*FESEM*): samples were studied by using a ZEISS ULTRA 55 microscope (Jena, Germany). For imaging samples were covered with gold and studied at 20 kV. Samples for chemical analysis (EDX) were not covered and studied at 15 kV.

Results and Discussion

BL and BLA

In the OM images (Figs. 3a, 3b), siliceous bodies (phytoliths) in BvL were identified in alignment. Two phytolith shapes were observed: the larger ones "saddle" and the smaller ones "dumbbell." The major axis of the phytoliths was perpendicular to the longitudinal axis of the leaf.

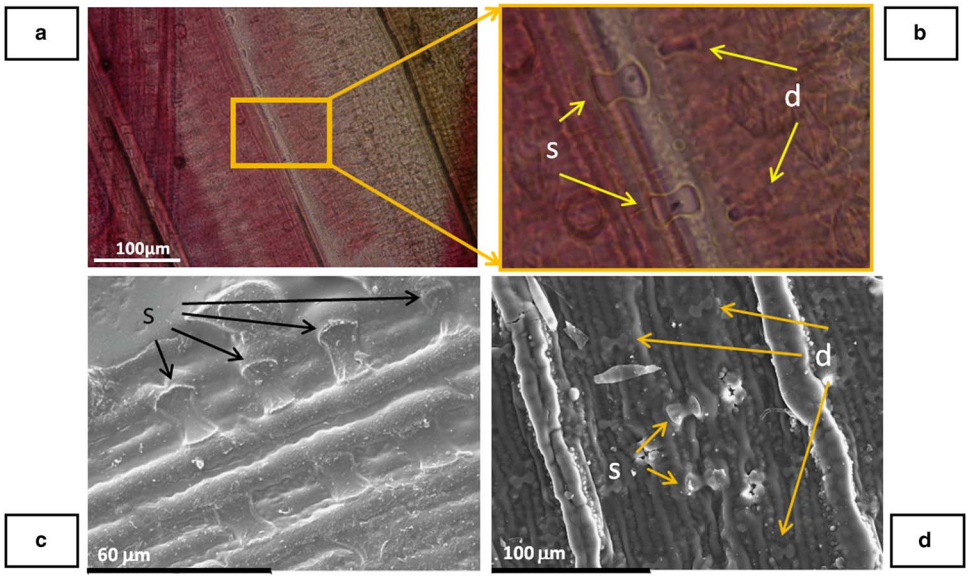

Figure 3. Images for bamboo leaf (BvL): (**a**) optical microscopy; (**b**) an enlarged zone of previous image; (**c**) cryo-SEM image for fresh leaf; (**d**) SEM image for dried leaf at 105°C. d, dumbbell phytolith; s, saddle phytolith; SEM, scanning electron microscopy.

In Figure 3c, the arrangement of the saddle phytoliths was clearly seen by the cryo-SEM technique, although no evidence of dumbbell phytoliths was found. A BvL leaf dried at 105°C (Fig. 3d) was studied by SEM: in this case, the relative positions of both phytolith types were also observed. EDX analysis (in atomic percentage) of the sample (carbon was not taken in this analysis) revealed a high proportion of Si and O (30.46 and 63.34%, respectively), but also important was the presence of three chemical elements: Ca (0.55%), K (3.74%), and Cl (1.91%). The presence of chloride and potassium is indicative of the presence of significant amounts of potassium chloride (KCl), probably originally accumulated in intracellular and extracellular fluids. These minerals, when drying, were deposited on the organic matter surface.

FESEM studies were carried out on BgL samples dried at 105°C. Selected micrographs are shown in Figure 4. They show the lower leaf surface (abaxial surface). The upper leaf surface (adaxial surface) was very homogeneous and it was very difficult to distinguish any structure because of the organic matter coating. In Figure 4a, a general view of the abaxial surface and aligned saddle phytoliths are distinguished. Figure 4b shows an enlargement in which dumbbell phytoliths are aligned together with "saddles" close to trichomes.

Bamboo leaves were calcined at different temperatures and the resulting ashes were analyzed by SEM (at 550 or 850°C, Fig. 5 for BvLA) and FESEM (450 or 650°C, Fig. 6 for BgLA). After treating at 550°C, the spodogram (structural residue resulting from the removal of organic matter by burning, maintaining the leaf's structure) was clearly observed (Fig. 5a, abaxial surface). The same type of arrangement as that found by means of OM was confirmed. Phytoliths of the two types were in a continuous matrix of an inorganic nature which results from the presence of silica and other minerals in the cell

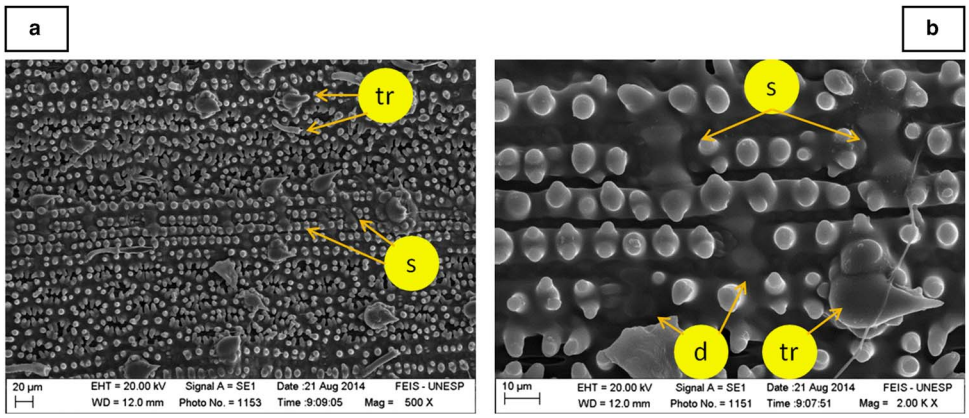

Figure 4. FESEM micrographs for BvL dried at 105°C: (**a**) general view of the abaxial surface; (**b**) enlarged zone. s, saddle; d, dumbbell; tr, trichome; FESEM, field emission scanning electron microscopy.

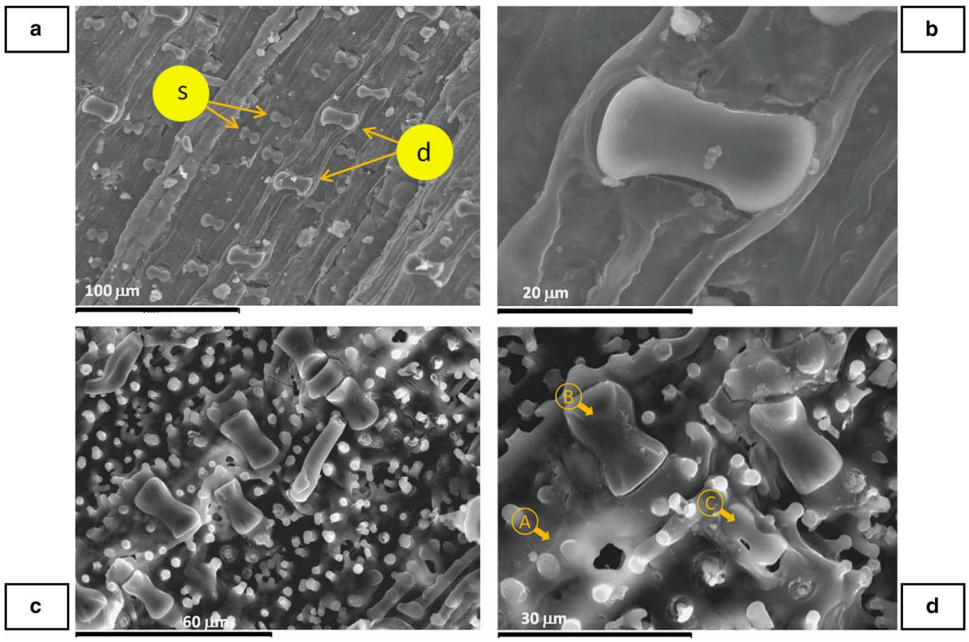

Figure 5. SEM micrographs for bamboo leaf ashes (BvLA): (**a**) calcined at 550°C; (**b**) saddle phytolith at 550°C; (**c**) at 850°C; (**d**) at 850°C, selected spots [(**a**) matrix; (**b**) saddle phytolith; (**c**) dumbbell phytolith] for chemical composition analysis (given in Table 1). d, dumbbell phytolith; s, saddle phytolith; SEM, scanning electron microscopy.

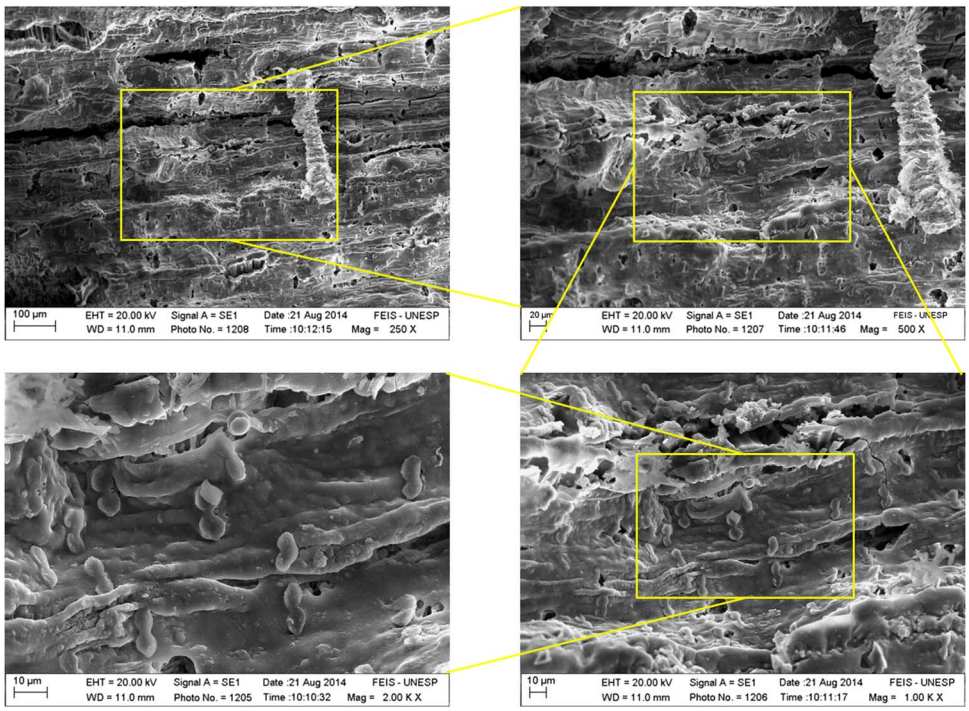

Figure 6. FESEM micrographs of adaxial surface for BvLA calcined at 650°C. FESEM, field emission scanning electron microscopy.

walls of the leaf. In this case, after removal of the organic matter, the chemical composition determined by EDX was: Si (23.33%), O (58.13%), K (11.77%), and Cl (3.40%). This means that after calcination at 550°C, potassium and chloride remained on the surface of the silica skeleton. Other minor components were also quantified: Ca (1.22%), P (0.84%), S (0.43%), and Mg (0.52%). Elemental analysis of saddle phytoliths (Fig. 5b) demonstrated their siliceous nature: Si (31.20%), O (64.18%), S (0.07%), Cl (1.38%), and K (3.18%).

The sample calcined at 850°C (Fig. 5c) still shows the spodogram, although in this case the inorganic material is

morphologically affected. The phytoliths remain nearly in their original position. Chemical composition for the overall sample is given in Table 1. From the chemical point of view, the EDX analysis comparison of samples treated at 550 and 850°C revealed that Si and O are the main elements, confirming the siliceous nature of the ash. However, significant differences were found in K and Cl content: for the sample calcined at 550°C the atomic percentages for these chemical elements were 11.77 and 3.40%, respectively, whereas for the sample at 850°C they were 1.77 and 0.04%. This leads to the conclusion that the temperature of 850°C produced a volatilization of KCl (its melting point is 776°C). The chemical composition of BvLA was not homogeneous, as can be seen in Figure 5d and in Table 1: Ca, P, S, and Mg were mainly concentrated in the matrix (Fig. 5d, spot A) that surrounded the phytoliths, having higher percentages of these elements than those found for the overall sample. In addition, K had the highest percentage for matrix (2.14%), which was higher than for the overall sample (1.77%), for saddle phytoliths (Fig. 5d, spot B), and dumbbell phytoliths (Fig. 5d, spot C). Chloride was found to be negligible in all the selected analysis spots.

Table 1. Chemical Compositions (Energy-Dispersive X-Ray, Atomic Percentage, %) for Bamboo Leaf Calcined at 850°C (BvLA) (Spots Identified in Fig. 5d).

Element	Overall	Matrix Spot A	Saddle Spot B	Dumbbell Spot C
Si	27.01	32.65	30.77	24.30
O	69.36	61.66	68.69	74.65
K	1.77	2.14	0.37	0.55
Cl	0.04	0.05	0.06	0.04
Ca	1.03	1.85	0.05	0.16
Mg	0.54	0.85	<0.01	0.24
P	0.15	0.49	<0.01	<0.01
S	0.14	0.18	<0.01	0.06

Table 2. Reported Chemical Composition for Bamboo Leaf Ashes (BLA) and BvLA (This Study).

		References				
	This Study (BvLA)	Dwivedi et al. (2006)	Frías et al. (2012)	Villar-cociña et al. (2011)	Iorliam et al. (2012)	Asha et al. (2014)
SiO_2	89.72	75.90	78.71	80.40	49.02	59.20
K_2O	4.61	5.62	3.78	1.33	10.10	ND
Cl	0.08	ND	ND	ND	ND	ND
CaO	3.19	7.47	7.82	5.06	9.89	ND
MgO	1.20	1.85	1.83	0.99	ND	0.54
P_2O_5	0.59	ND	0.99	0.56	3.80	ND
SO_3	0.62	1.06	1.00	1.07	1.00	1.40
Loss on ignition	ND	ND	3.83	8.04	25.00	11.20

Some chemical analyses have been reported for BLA (Dwivedi et al., 2006; Singh et al., 2007; Villar-Cociña et al., 2011; Frías et al., 2012; Iorliam et al., 2012; Asha et al., 2014). In them, silicon dioxide was the major compound (see Table 2), and a similar percentage of SiO_2 was found for the overall analysis in this study. The lowest SiO_2 data (Iorliam et al., 2012; Asha et al., 2014) were found for samples with a high loss on ignition (LOI) parameter (this LOI showed that the calcinations were far from completed). However, no data on the chloride percentage was supplied in any previous report. Yet, this fact is important for the application of this type of ash in the manufacture of cements and concretes: chloride content should be taken into account in order to assess the possible reinforcement corrosion.

According to the data presented in Table 1, it is evident that there is a wide variety of structures with different chemical composition, undoubtedly attributed to the differentiated tissues and cells. Thus, in order to make an overall analysis by means of EDX measurements, chemical compositions were taken from 16 tests on BgLA calcined at 850°C. The analysis was carried out by analyzing a $115 \times 85\ \mu m$ area: from the 16 tests, mean values and their standard deviations were measured (see Table 3). It is confirmed that volatilization of chlorides took place due to the high calcination temperature, finding chloride content in the 0.26–0.0% range (mean value of 0.07%). Mean SiO_2 content was 88.58%, which was very similar to that found in BvLA. In a few tests, small amounts of Al_2O_3 and Fe_2O_3 were identified, which was attributed to the presence of soil particles adhered to the leaves.

In Figure 6 the spodogram of the adaxial surface for BgLA (650°C) is observed. In this part of the calcined leaf, only dumbbell phytoliths were identified, surrounded by a smoother silica matrix. This matrix was very porous, indicating that the silica content in most of the cells

Table 3. Mean Values of Chemical Composition for BgLA Calcined at 850°C.

	SiO_2	K_2O	Cl	CaO	MgO	P_2O_5	SO_3	Al_2O_3	Fe_2O_3	Na_2O
Mean value	88.58	5.59	0.07	2.70	0.79	0.85	1.01	0.10	0.13	0.16
SD	3.87	1.73	0.07	1.29	0.44	0.79	0.34	0.19	0.33	0.21
Maximum value	94.61	8.21	0.26	4.79	1.69	2.49	1.59	0.48	1.15	0.72
Minimum value	83.00	2.35	0.00	0.78	0.30	0.00	0.00	0.00	0.00	0.00

Values were calculated from energy-dispersive X-ray analysis on $115 \times 85\ \mu m$ zone (16 tests were carried out).

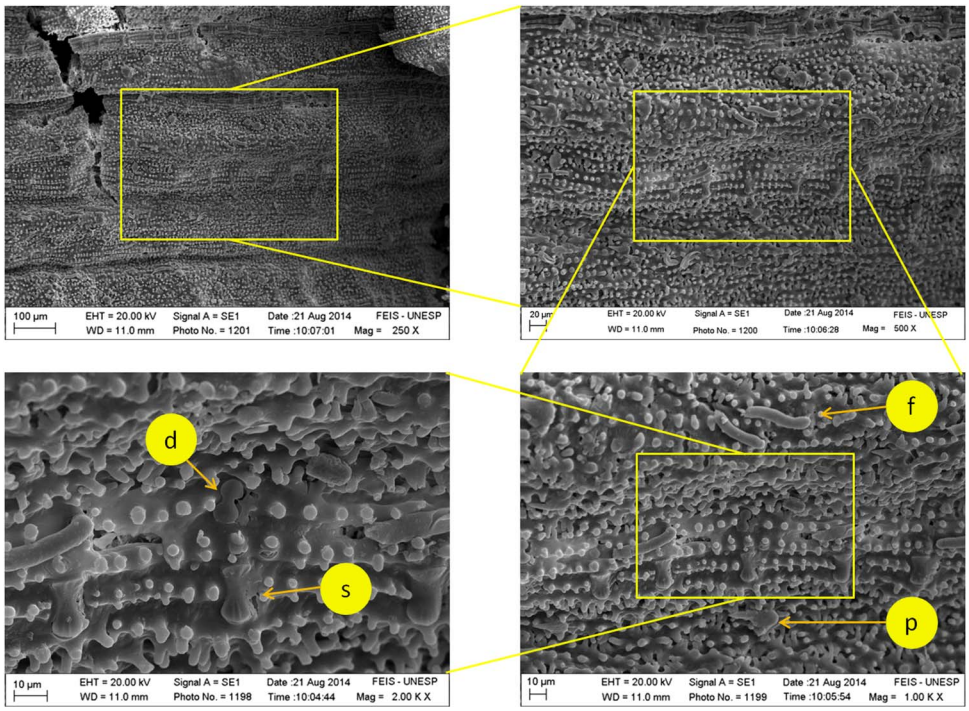

Figure 7. FESEM micrographs of abaxial surface for BvLA calcined at 650°C. p, prickle hairs; f, filiformed hairs; d, dumbbell phytolith; s, saddle phytolith; FESEM, field emission scanning electron microscopy.

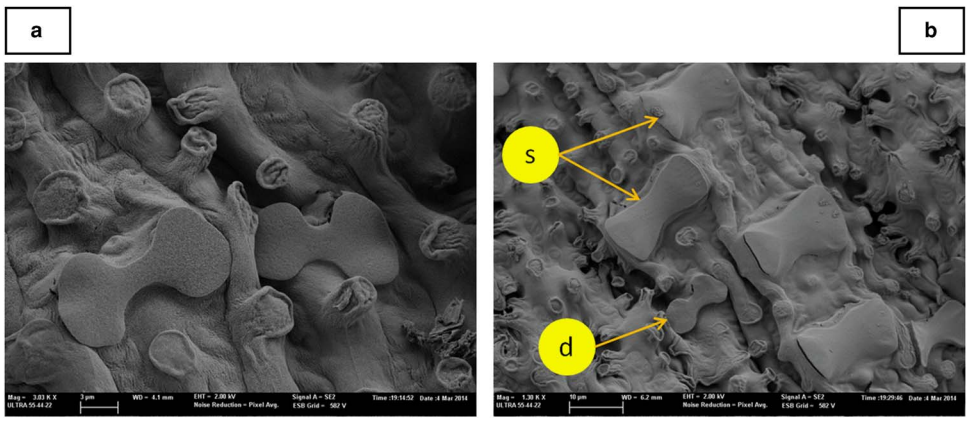

Figure 8. FESEM micrographs for BgLA at 850°C: (**a**) dumbbell phytoliths; (**b**) dumbbell (d), and saddle (s) phytoliths. FESEM, field emission scanning electron microscopy.

was lower than that found in the phytolitic specialized single cells. By contrast, the abaxial surface (Fig. 7) showed another arrangement: saddle and dumbbell phytoliths are aligned, surrounded by rough silica matrix, in which two types of trichomes (prickle hairs, filiformed hairs) are identified (Motomura et al., 2006).

Phytoliths were better observed on samples calcined at 850°C. FESEM micrographs for BgLA are shown in Figure 8. The saddle and dumbbell phytoliths in BvLA were similar to those found in BgLA. Saddle phytoliths were 16–20 μm long and 9–12 μm wide, whereas dumbbell phytoliths were 10–15 μm long and 6–7 μm wide.

SL and SLA

In Figure 9, several images of SL are shown. In Figure 9a, with OM, the general arrangement of cellular elements of the epidermis is observed. Dumbbell type phytoliths are aligned and arranged so that the major axis thereof is parallel to the major axis of the epidermal cells. Figure 9b shows an enlarged image in which some dark inclusions in the phytoliths are identified, probably related to the carbon sink mentioned previously (Li et al., 2014). Figures 9c and 9d show these inclusions and also the variability of shapes for dumbbell phytoliths (Gallego & Distel, 2004): the phytolith

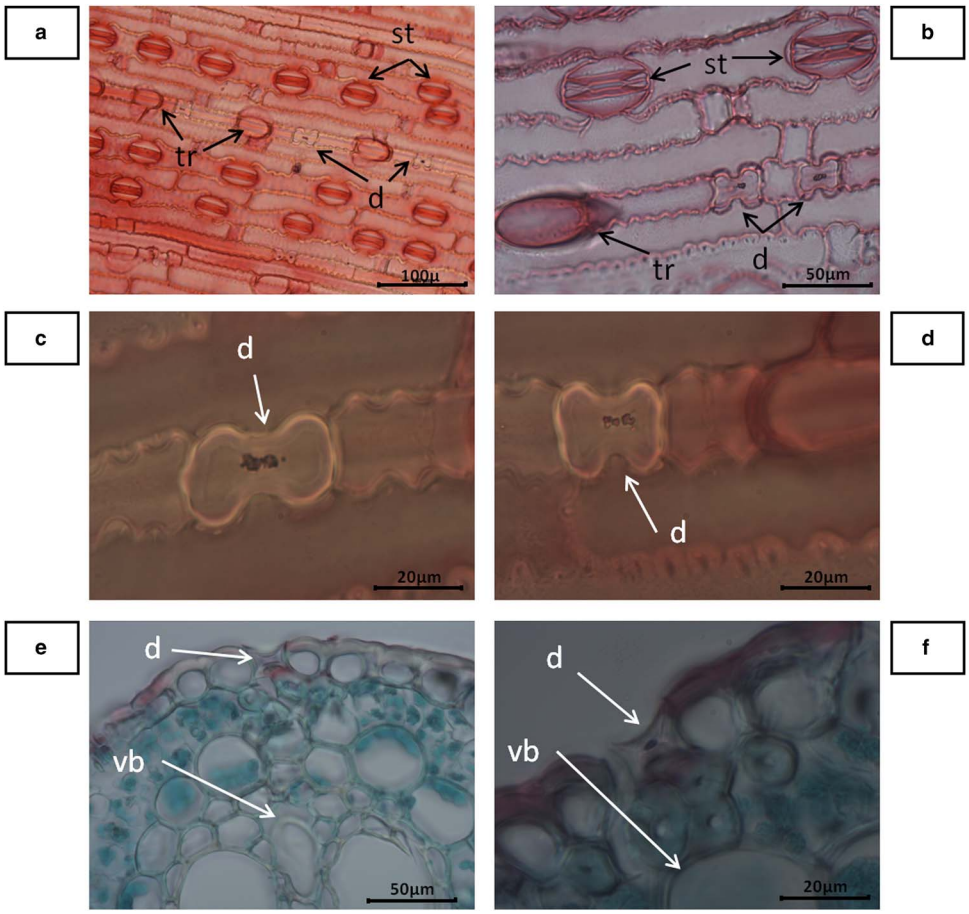

Figure 9. Optical microscope images for sugarcane leaves: (**a**–**d**) paradermal sections; (**e**, **f**) transversal sections. d, dumbbell phytolith; st, stoma; tr, trichoma; vb, vascular bundles.

in Figure 9c shows a short shank-convex end, and the phytolith in Figure 9d shows a short shank-straight end. The cross-section of SL is observed in Figures 9e and 9f. It can be seen that the phytolith is situated on the vascular bundles (Motomura et al., 2006) and the phytolith section was a trapezoid-like shape.

Cryo-SEM images (Fig. 10) were taken to identify the disposition of phytoliths in sugarcane leaf (SL). Figure 10a shows a cross-section of the leaf, in which a phytolith in the abaxial surface was situated in a similar position to those found in Figures 9e and 9f, among the epidermis cells and on the vascular bundle. Figure 10b shows an enlargement image of the selected zone: a trapezoidal shape was observed for the phytolith. Interesting detail of the panicoide dermotype is identified in Figure 10c. The chemical composition determined by EDX has a lower proportion of Si (5.18%) compared with O (88.10%); moreover, the presence of other chemical elements in relevant quantities, such as Cl (3.15%), K (2.90%), Mg (0.26%), P (0.18%), and S (0.23%) was found. It can be noticed that the inorganic residue was very different from the case of BL: for SL, the silica skeleton was under the organic coating and the amount of phytoliths was lower, and consequently the relative proportion of silicon was reduced. Finally, Figure 10d clearly shows phytoliths of the dumbbell type, which appeared in the surface of the leaf.

FESEM studies on SL dried at 105°C showed that the adaxial surface did not present any identifiable phytoliths. However, in the abaxial surface there were silica cells (Fig. 11a). It was possible to identify different morphologies for dumbbell phytoliths (Figs. 11b–11d) and their length/width ratio varied significantly.

Calcination of SL generates SLA, in which the resulting material tends to be completely disordered, as can be seen in Figure 12: the cellular leaf structure tissues (spodogram) are not maintained when organic matter is removed by combustion. In Figure 12 two SEM micrographs of SLA obtained at 450°C reflected this behavior. In the first one (Figure 12a), a lot of small particles of irregular shapes and some cellular structures still maintaining their original structure (stomata and phytoliths) were observed. In Figure 12b, a dumbbell phytolith was surrounded by irregular particles. The chemical composition of the ash revealed again the low proportion of silicon compared with other chemical elements: Si (5.24%), O (72.14%), Mg (4.53%), Cl (2.61%), K (8.81%), P (2.37%), S (0.85%), and Ca (3.25%). Probably the low Si content, and that of

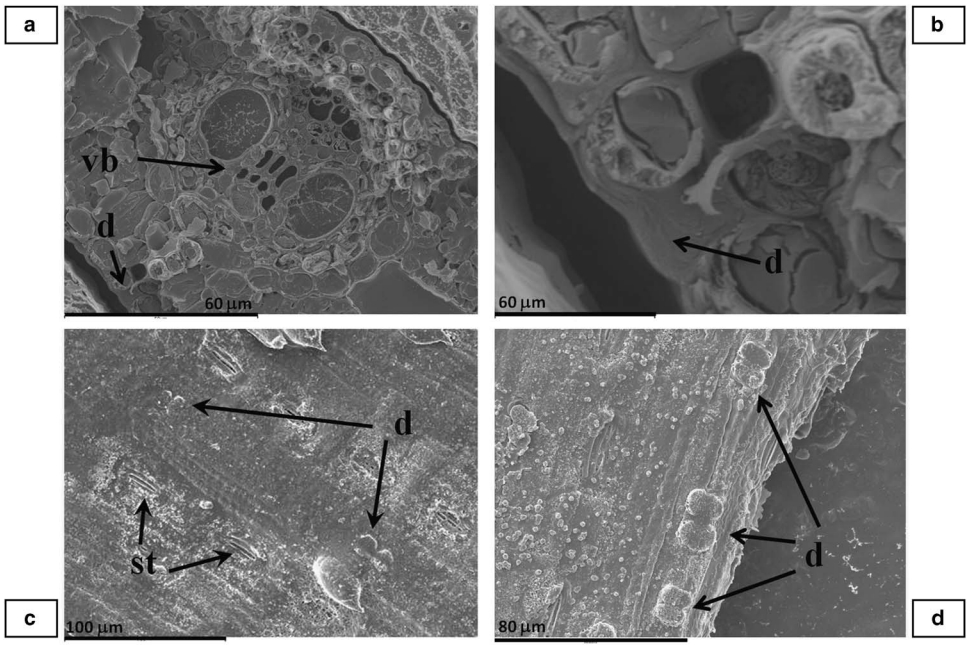

Figure 10. Cryo-SEM micrographs for sugarcane leaf: (**a**, **b**) cross-section; (**c**, **d**) abaxial surface. d, dumbbell phytolith; st, stoma; vb, vascular bundle; SEM, scanning electron microscopy.

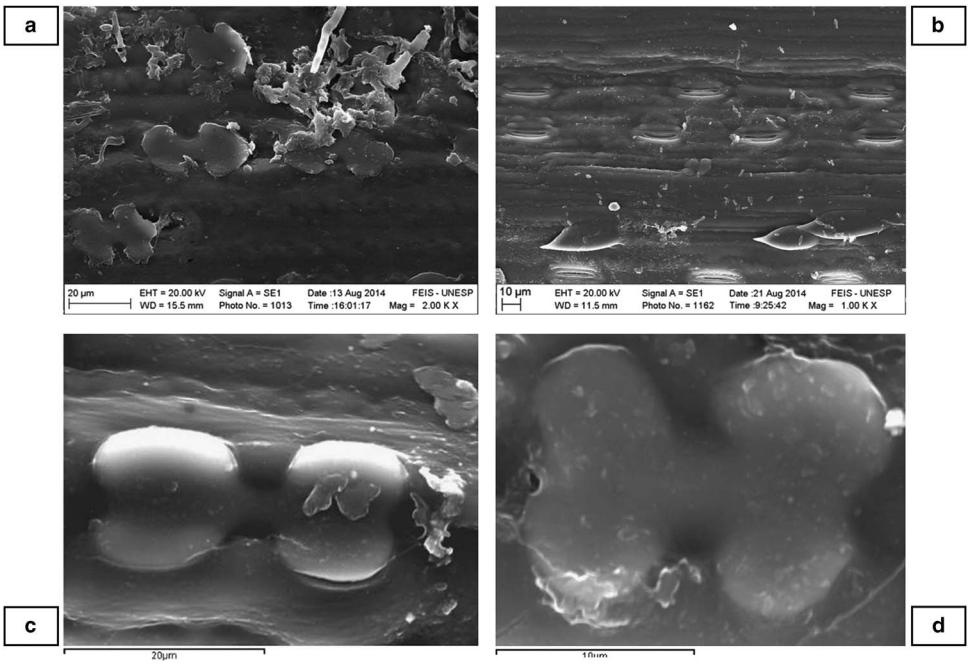

Figure 11. Micrographs of SL dried at 105°C: (**a**, **b**) FESEM; (**c**, **d**) SEM. SL, sugarcane leaf; FESEM, field emission scanning electron microscopy; SEM, scanning electron microscopy.

silica, makes it impossible to maintain the spodogram after calcination. In Figure 12b detail of a dumbbell phytolith is shown: its chemical composition was very rich in silica: Si (25.89%), O (71.13%), Cl (0.19%), K (2.61%), Mg (0.12%), and S (0.06%). This means that a significant proportion of silica in the ash is concentrated in phytoliths remaining after calcination.

On the micrographs shown in Figures 12a and 12c, selected chemical analyses (spots and zones) were obtained by EDX. In Figure 13 these spots and zones are marked and the corresponding chemical analysis is summarized in Table 4. As occurs for bamboo ashes, a wide range of chemical composition was found depending on the spot/zone selected. Analysis of the phytoliths yielded the highest

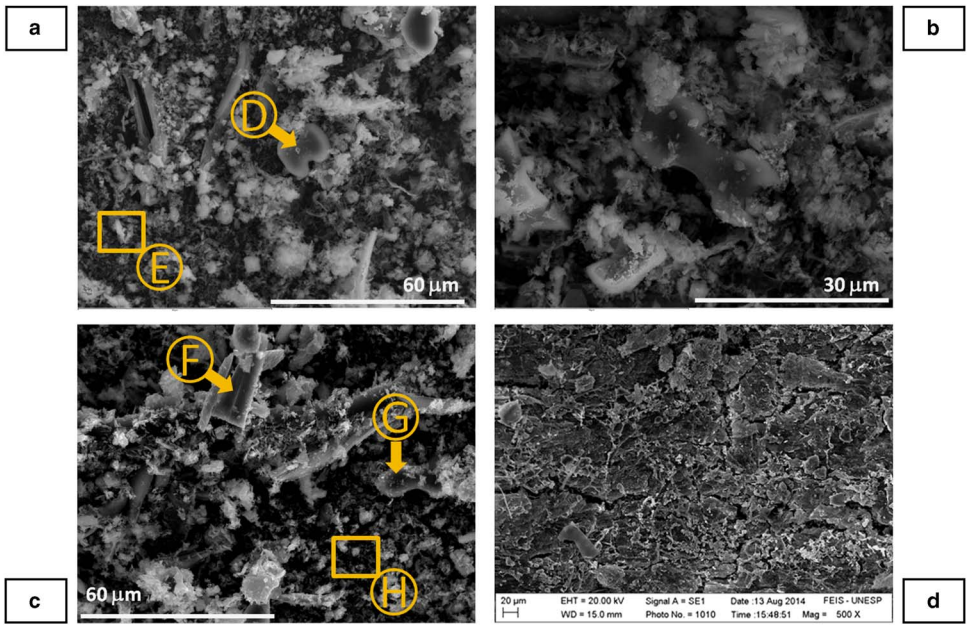

Figure 12. Micrographs for SLA calcined at 450°C: (**a**) SEM general view with D spot and E zone; (**b**) detail of dumbbell phytolith; (**c**) SEM general view with F and G spots and H zone; (**d**) FESEM general view. Chemical composition from spots and zones are given in Table 4. SLA, sugarcane leaf ash; SEM, scanning electron microscopy; FESEM, field emission scanning electron microscopy.

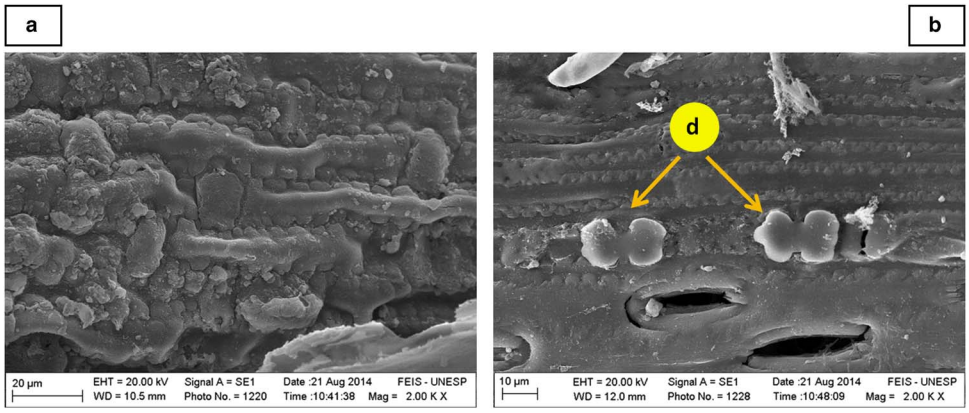

Figure 13. FESEM micrographs for SLA calcined at 350°C: (**a**) adaxial surface; (**b**) abaxial surface. d, dumbbell phytolith; FESEM, field emission scanning electron microscopy; SLA, sugarcane leaf ash.

Si content (spots D and G), whereas K, Cl, Ca, Mg, P, and S contents were significantly lower than those found for the other zones/spots. In order to analyze in depth the chemical composition of SLA by means of EDX tests, 14 tests on SLA obtained at 650°C were taken. Analyses were carried out on a $115 \times 85\ \mu m$ area: from the 14 tests, mean values and their standard deviations were measured (see Table 5). SiO_2 and K_2O are the major compounds in the ash: the presence of a high percentage of potassium could be a problem when the ash is added to concrete mix because of the alkali–silica reaction: it is well-known (Diamond, 1975), that the presence of alkalis in the Portland cement matrix can produce an expansive reaction when reacted towards specific types of aggregates. Opal aggregates react with alkalis to form expansive sodium silicate gel (N-S-H) in the aggregate–matrix

Table 4. Chemical Compositions (Energy-Dispersive X-Ray, Atomic Percentage, %) for Sugarcane Leaf Ash Calcined at 450°C (Spots and Zones Identified in Fig. 12).

	Figure 12a			Figure 12c		
Element	Overall	Spot D	Zone E	Spot F	Spot G	Zone H
Si	5.24	25.89	4.14	0.84	39.16	3.67
O	72.14	71.13	73.27	47.71	52.14	72.09
K	8.81	2.61	9.93	16.88	7.71	9.38
Cl	2.61	0.19	2.23	0.48	0.32	4.91
Ca	3.25	<0.01	2.25	<0.01	<0.01	1.91
Mg	4.53	0.12	4.76	11.39	0.34	5.40
P	2.37	<0.01	2.46	22.29	0.23	1.90
S	0.85	0.06	0.96	0.21	0.09	0.73

Table 5. Mean Values of Chemical Composition for Sugarcane Leaf Ash Calcined at 450°C.

	SiO_2	K_2O	Cl	CaO	MgO	P_2O_5	SO_3	Al_2O_3	Fe_2O_3	Na_2O
Mean value	29.95	29.05	3.95	14.76	9.81	5.76	6.14	0.32	0.12	0.15
SD	14.56	6.46	1.62	9.00	4.38	3.41	2.63	0.61	0.33	0.22
Maximum value	60.25	40.18	6.65	25.04	14.50	10.64	9.79	2.19	1.15	0.49
Minimum value	7.72	20.29	1.91	0.00	1.41	0.00	1.28	0.00	0.00	0.00

Values were calculated from energy-dispersive X-ray analysis on 115 ×85 μm zone (14 tests were carried out).

Table 6. Reported Chemical Composition for Sugarcane Leaf Ashes (SLA) and SLA (This Study).

		References					
	This Study	Frías et al. (2007)	Singh et al. (2009)	Le Blond et al. (2010)	Guzmán et al. (2011)	Arumugam et al.. (2012)	Rodrigues et al. (2013)
SiO_2	29.95	70.20	74.79	20.20–24.77	81.00	80.14	61.00
K_2O	29.05	3.05	2.37	7.64–8.84	3.00	3.09	7.00
Cl	3.95	ND	ND	ND	ND	0.67	0.6
CaO	14.76	12.20	6.39	1.34–1.58	6.00	6.06	4.40
MgO	9.81	1.95	2.42	8.58–9.83	2.00	5.02	2.80
P_2O_5	5.76	1.40	ND	1.70–3.00	1.10	ND	2.30
SO_3	6.14	4.10	1.36	ND	1.40	2.25	3.90
Loss on ignition	ND	1.81	ND	30.00–31.20	4.00	ND	2.10
Al_2O_3	0.32	1.93	5.03	3.87–5.59	0.6	0.89	9.20
Fe_2O_3	0.12	2.09	4.46	1.92–3.29	0.7	0.51	5.00

interface (Diamond, 1976). Thus, some adjustments may need to be taken into account when these SLAs replace Portland cement in concrete if reactive aggregates are used. The obtained chemical compositions in this study were very different from those reported previously, as can be seen in Table 6. The reported values were probably taken from samples of a mixture of leaves, straw, sugarcane, and soil, and consequently a higher silica proportion was obtained. In addition, percentages of Al_2O_3 and Fe_2O_3 in reported data (Frías et al., 2007; Singh et al., 2009; Le Blond et al., 2010; Guzmán et al., 2011; Arumugam et al., 2012; Rodrigues et al., 2013) were very high due to the soil contamination of the leaves/straw, unlike the very low values for these oxides in the studied ash in this study, which were below 0.5% because the calcined leaves were previously washed with deionized water.

In order to maintain the skeleton of the tissues, SL was calcined at 350°C. At this temperature the organic matter was not completely removed, so the residual organics and/or carbon together with the silica helped to maintain the original structure of the cells. In Figure 13, FESEM micrographs of the obtained material are shown. In the adaxial surface, no evidence of the presence of phytoliths is obtained (Fig. 13a), whereas for the abaxial surface (Fig. 13b) phytoliths were arranged according to the observations at 105°C.

In Figure 14, a complete arrangement of the phytoliths is observed after calcination at 350°C. In this case, because part of the organic matter was removed, the identification of these silica structures was easier than for the sample dried at 105°C.

Conclusions

Microscopy studies have shown the presence of phytoliths (silica cells) in BL and SL. A higher proportion of silica in the cell walls of BL was observed than in SL.

The arrangement and type of phytoliths (dumbbell and saddle) is characteristic of each type of leaf: phytoliths were aligned parallel to the longitudinal axis of the cells for SL (panicoide type) and aligned transversely for BL (bambusoide type).

BLA: (BvLA from *B. vulgaris* and BgLA from *B. gigantea*) presented significant amounts of K and Cl, and SLAs have important amounts of other chemical elements: Mg, Ca, P, and S. A reduction of chloride percentage was observed when ashes were obtained at high temperature (850°C), due to the volatilization of KCl.

The silica content in the ash is directly related to the formation of the spodogram after calcination. For SLA, which has the lowest silica content, the cell structure practically collapses after calcination. However, a perfect spodogram for BLA was maintained at 850°C.

The phytoliths characterized in both ashes (BLA and SLA) had a very high content of silica. Other elements were presented in the inorganic matter after calcination. For BLA, silica was the main compound, while for SLA significant percentages of K_2O, Cl, CaO, MgO, P_2O_5, and SO_3 were found. EDX chemical analysis demonstrated that the chemical composition varied depending on the particle or zone analyzed.

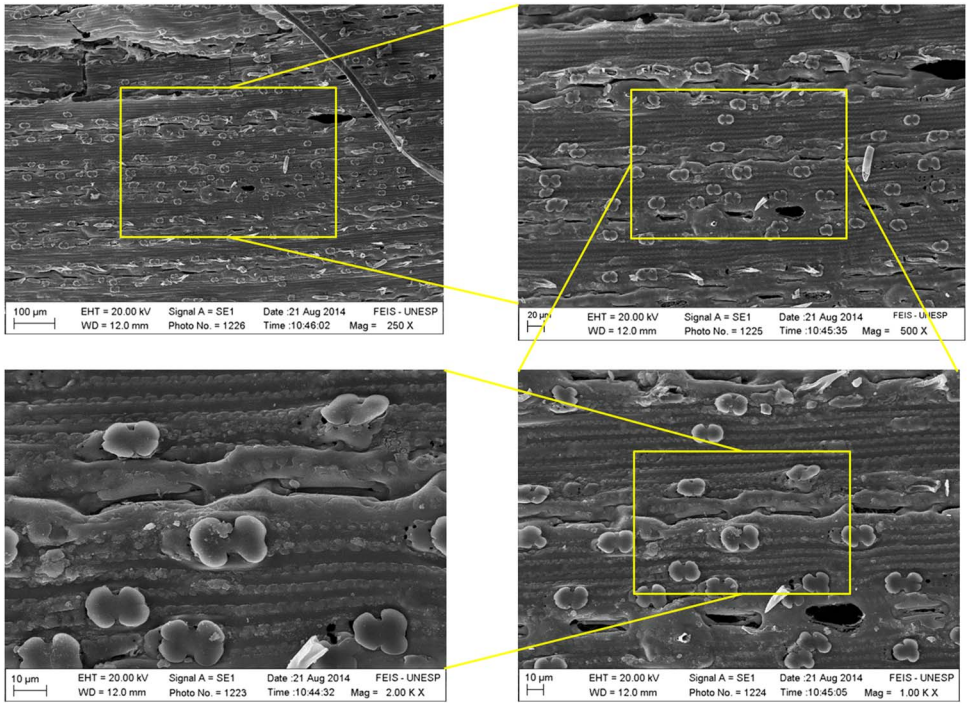

Figure 14. FESEM micrographs of abaxial surface for SLA calcined at 350°C. FESEM, field emission scanning electron microscopy; SLA, sugarcane leaf ash.

These ashes are materials that can be used for the manufacture of cement and concrete, although account must be taken of the presence of K and Cl, which may limit their applications. Potassium could generate expansive problems by alkali–silica reaction with reactive aggregates, and chloride could lead to corrosion processes in steel-reinforced concrete.

Acknowledgments

The authors thank the Conselho Nacional de Desenvolvimento Científico e Tecnológico (Projeto CNPq 40174/2013-1) of Brazil for funding the research. The authors thankthe Electron Microscopy Service of the Universitat Politècnica de València and Materials Department of Universidade Estadual Paulista at Ilha Solteira.

References

Aprianti, E., Shafigh, P., Bahri, S. & Farahani, J.N. (2015). Supplementary cementitious materials origin from agricultural wastes – A review. *Constr Build Mater* **74**, 176–187.

Arumugam, A. & Ponnusami, V. (2012). Modified SBA-15 synthesized using sugarcane leaf ash for nickel adsorption. *Indian J Chem Technol* **20**, 101–105.

Asha, P., Salman, A. & Kumar, R.A. (2014). Experimental study on concrete with bamboo leaf ash. *Int J Eng Adv Technol* **3**, 46–51.

Diamond, S. (1975). A review of alkali-silica reaction and expansion mechanisms 1. Alkalis in cements and in concrete pore solutions. *Cem Concr Res* **5**, 329–345.

Diamond, S. (1976). A review of alkali-silica reaction and expansion mechanisms 2. Reactive aggregates. *Cem Concr Res* **6**, 549–560.

Dwivedi, V.N., Singh, N.P., Das, S.S. & Singh, N.B. (2006). A new pozzolanic material for cement industry: Bamboo leaf ash. *Int J Phys Sci* **1**, 106–111.

Epstein, E. (1999). Silicon. *Annu Rev Plant Physiol Plant Mol Biol* **50**, 641–664.

Erra, G., Zucol, A.F. & Kröhling, D.M. (2011). Phytolitic analysis of the Tezanos Pinto Formation (Late Pleistocene–early Holocene) in the northwestern sector of its distribution area, Provincia de Entre Ríos (Argentina). *Rev Mex Cienc Geol* **28**, 398–412.

Frías, M., Savastano, H., Villar, E., Sánchez De Rojas, M.I. & Santos, S. (2012). Characterization and properties of blended cement matrices containing activated bamboo leaf wastes. *Cem Concr Comp* **34**, 1019–1023.

Frías, M., Villar-Cociña, E. & Valencia-Morales, E. (2007). Characterisation of sugar cane straw waste as pozzolanic material for construction: Calcining temperature and kinetic parameters. *Waste Manag* **27**, 533–538.

Gallego, L. & Distel, R.A. (2004). Phytolith assemblages in grasses native to central Argentina. *Ann Bot* **94**, 865–874.

Guzmán, A., Gutiérrez, C., Amigó, V., De Gutiérrez, R.M. & Delvasto, S. (2011). Pozzolanic evaluation of the sugar cane leaf. *Mater Constr* **61**, 213–225.

Hosseini, M.M., Shao, Y. & Whalen, J.K. (2011). Biocement production from silicon-rich plant residues: Perspectives and future potential in Canada. *Biosyst Eng* **110**, 351–362.

Iorliam, A.Y., Agbede, I.O. & Joel, M. (2012). Effect of bamboo leaf ash on cement stabilization of Makurdi shale for use as flexible pavement construction material. *Am J Sci Ind Res* **3**, 166–174.

Kamenik, J., Mizera, J. & Randa, Z. (2013). Chemical composition of plant silica phytoliths. *Environ Chem Lett* **11**, 189–195.

Le Blond, J.S., Horwell, C.J., Williamson, B.J. & Oppenheimer, C. (2010). Generation of crystalline silica from sugarcane burning. *J Environ Monit* **12**, 1459–1470.

Le Blond, J.S., Williamson, B.J., Horwell, C.J., Monro, A.K., Kirk, C.A. & Oppenheimer, C. (2008). Production of potentially hazardous respirable silica airborne particulate from the burning of sugarcane. *Atmos Environ* **42**, 5558–5568.

Li, B., Song, Z., Wang, H., Li, Z., Jiang, P. & Zhou, G. (2014). Lithological control on phytolith carbon sequestration in mosobamboo forests. *Sci Rep* **4**, 5262, 5pp.

Ma, J.F. & Yamaji, N. (2006). Silicon uptake and accumulation in higher plants. *Trends Plant Sci* **11**, 392–397.

Mehta, P.K. (1989). *Pozzolanic and Cementitious By-Products in Concrete: Another Look* (ACI Special Publication). Farmington Hills, MI, USA: American Concrete Institute. pp. 1–44.

Mohapatra, S., Sakthivel, R., Roy, G.S., Varmac, S., Singh, S.K. & Mishra, D.K. (2011). Synthesis of β-SiC powder from bamboo leaf in a DC extended thermal plasma reactor. *Mater Manuf Processes* **26**, 1362–1368.

Motomura, H., Fujii, T. & Suzumi, M. (2006). Silica deposition in abaxial epidermis before the opening of leaf blades of Pleioblastus chino (Poaceae, Bambusoideae). *Ann Bot* **97**, 513–519.

Neethirajan, S., Gordon, R. & Wang, L. (2009). Potential of silica bodies (phytoliths) for nanotechnology. *Trends Biotechnol* **27**, 461–467.

Nzihou, A. (2010). Toward the valorization of waste and biomass. *Waste Biomass Valoriz* **1**, 3–7.

Payá, J., Monzó, J. & Borrachero, M.V. (2010). Outstanding aspects on the use of rice husk ash and similar agrowastes in the preparation of binders. In *Proceedings of the First Pro-Africa Conference: Non Conventional Building Materials Based on Agroindustrial Wastes*, Savastano Jr. H. (Ed.), pp. 179–181). São Paulo, Brazil: Pirassununga.

Prat, H. (1936). La Systematique des Graminées. *Ann Sci Nat* **18**, 165–258.

Prychid, C.J., Rudall, P.J. & Gregory, M. (2003). Systematics and biology of silica bodies in monocotyledons. *Bot Rev* **69**, 377–440.

Rodrigues, M.S., Beraldo, A.L., Savastano, J.R.H. & Santos, S.F. (2013). Sugarcane straw ash as mineral addition in fibercement. *Rev Bras Eng Agric Amb* **17**, 1347–1354.

Santos, S.F., Tonoli, G.H.D., Mejia, J.E.B., Fiorelli, J. & Savastano, H. Jr. (2015). Non-conventional cement-based composites reinforced with vegetable fibers: A review of strategies to improve durability. *Mater Constr* **65**, e041.

Singh, N.B., Das, S.S., Singh, N.P. & Dwivedi, V.N. (2009). Studies on SCLA composite Portland cement. *Indian J Eng Mater Sci* **16**, 415–422.

Singh, N.B., Dasa, S.S., Singh, N.P. & Dwivedi, V.N. (2007). Hydration of bamboo leaf ash blended Portland cement. *Indian J Eng Mater Sci* **14**, 69–76.

Teixeira, S.R., Souza, A.E., Carvalho, C.L., Reynoso, V.C.S., Romero, M. & Rincón, J.M. (2014). Characterization of a wollastonite glass-ceramic material prepared using sugar cane bagasse ash (SCBA) as one of the raw materials. *Mater Charact* **98**, 209–214.

Tuck, O.C., Pérez, E., Horváth, I.T., Sheldon, R.A. & Poliakoff, M. (2012). Valorization of biomass: Deriving more value from waste. *Science* **237**, 695–699.

Villar-Cociña, E., Morales, E.V., Santos, S.F., Savastano, H. Jr. & Frías, M. (2011). Pozzolanic behavior of bamboo leaf ash: Characterization and determination of the kinetic parameters. *Cem Concr Comp* **33**, 68–73.